

Magnetic Field Configuration Dependence of Plasma Production and Parallel Transport in a Linear Plasma Device NUMBER^{*)}

Daichi HAMADA, Atsushi OKAMOTO, Takaaki FUJITA, Hideki ARIMOTO, Katsuya SATOU and Ryosuke OCHIAI

Graduate School of Engineering, Nagoya University, Furo-cho, Chikusa-ku, Nagoya 464-8603, Japan

(Received 28 December 2017 / Accepted 14 March 2018)

In order to study a new method of generating energetic ion, a linear plasma device NUMBER was designed and constructed. The device consists of a plasma production region and a test region connected axially. The radial profile of the electron density and the electron temperature were measured using a Langmuir probe. The radius of plasma is consistent with a field line trace calculation. The time evolution of the ion saturation current I_{is} was measured. A high I_{is} phase accompanied by rapid increase and rapid decrease of I_{is} was observed. From the scan of magnetic field in the test region, it is found that the high I_{is} phase may be caused by unexpected electron cyclotron resonance in the test region. The gas pressure is also related to the appearance of the high I_{is} phase.

© 2018 The Japan Society of Plasma Science and Nuclear Fusion Research

Keywords: energetic ion, linear plasma device, electron cyclotron resonance, overdense plasma, plasma production

DOI: 10.1585/pfr.13.3401044

1. Introduction

Alpha particles are expected to heat plasma by transferring their energy. Confining the alpha particles is necessary to keep the high temperature plasma. Therefore, study on the alpha particle transport is very important in magnetically confined nuclear fusion.

Stellarators have various magnetic field configurations. Therefore it is necessary to investigate the performance of the alpha particle confinement on the stellarators with various configurations. Neutral beam injection (NBI) is usually used to produce energetic ions. However, since this method utilizes ionization and charge exchange interaction, flexibility of this method depends on the fixed beam line and ionization point. Therefore, a new method of generating energetic ions applicable to stellarators, especially small ones, is required for alpha particle study.

A linear plasma device NUMBER (Nagoya University Magnetoplasma Basic Experiment) was designed and constructed to develop a new method of generating energetic ions. Target values of the electron density and the electron temperature are $\sim 1 \times 10^{18} \text{ m}^{-3}$ and $\sim 10 \text{ eV}$, respectively, corresponding to those achieved in small stellarators [1–4]. Other requirements for the device are a uniform magnetic field of about 0.3 T and a large ($> 0.05 \text{ m}$) diameter of plasma column. The requirement of magnetic field strength comes from feasibility studies of the energetic ion production method in magnetic field strength similar to that of the small stellarators. The diameter of the plasma column is determined from the Larmor radius of

energetic ion, the energy of which is chosen so that normalized energy to bulk ion temperature is the same order to that in a fusion reactor. These parameters are important for understanding extraction mechanism of the energetic ion.

In order to achieve these density, temperature, and diameter, an overdense plasma production method [5] is adopted for the linear device. The plasma is produced by the electron cyclotron resonance (ECR) with a microwave injected along the magnetic field. While the magnetic field strength is constrained by a microwave frequency of commercially available power source, 0.0875 T for 2.45 GHz, the requirement on the magnetic field strength is rather higher. Therefore a connected linear device, which consists of a lower magnetic field ECR plasma production region followed by a higher field test region, was proposed. After fabrication and commissioning was finished, this device was transferred from Tohoku University to Nagoya University in the spring of 2016. We started the experiment from the fall of 2016. To achieve these plasma parameters, we studied the magnetic field configuration dependence of plasma production and parallel transport in NUMBER.

2. Experimental Setup

NUMBER has a plasma production region and a test region. The new method of energetic ion production will be evaluated in the test region. Dimensions of the vacuum chamber are 1.8 m in length and 0.2 m in diameter. The frequency and injection power of a microwave power source for ECR plasma production are 2.45 GHz and 6.0 kW, respectively. To produce the overdense plasma, the magnetic field in the production region is a magnetic beach configu-

author's e-mail: okamoto.atsushi@nagoya-u.jp

^{*)} This article is based on the presentation at the 26th International Toki Conference (ITC26).

ration [5]. The magnetic field in the test region is generated by a ~ 20 kJ capacitor bank while that in the production region is kept constant by a ~ 8 kW DC power supply. A steady state plasma is produced and maintained with the magnetic beach in the production region. When the field is generated in the test region, it is expected that the plasma is transported from the production region to the test region along the field lines. The experimental setup and the magnetic field configuration are shown in Fig. 1. The red curve indicates the magnetic field generated by a DC power supply. The blue curve indicates the magnetic field generated by a capacitor bank. The black curve indicates the total magnetic field. The magnetic field for ECR with 2.45 GHz microwave, 0.0875 T is shown by an yellow dotted line.

Power supply circuit for generating magnetic field in the test region is shown in Fig. 2 (a). Two capacitors are connected in parallel through an inductor, and the switches are turned on by shifting the timing. Ignitrons are used as the switches. Time evolution of magnetic field coil current (I_{MCT}) and that of magnetic field strength (B_{MCT}) in the test region are shown in Fig. 2 (b). A negative spike ($t = 16$ ms) is caused by a stray inductance of crowbar circuit and results in open of main circuit. Flat top time of the magnetic field in the test region is about 4 ms, which was defined as the time that magnetic field strength changes within $\pm 1\%$

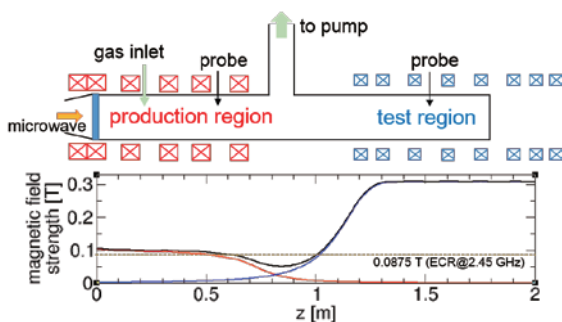


Fig. 1 Schematic of the experimental setup and magnetic field configuration in the NUMBER device.

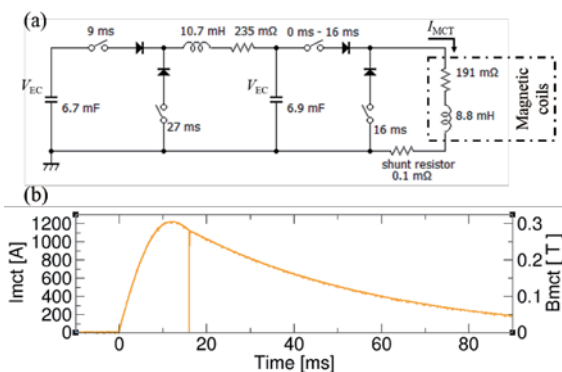


Fig. 2 (a) Power supply circuit for generating magnetic field in the test region. (b) Time evolution of magnetic field coil current and that of magnetic field strength in the test region for $V_{EC} = 1600$ V.

around the peak. Then 0.3 T of magnetic field is generated uniformly about 1 m in axial length. When the charging voltage of capacitor bank (V_{EC}) is 1600 V, the magnetic field strength becomes 0.3 T at the peak of waveform ($t = 13$ ms). Helium gas is used in the experiment. Operation pressure is 0.19 Pa, except for a gas pressure scanning experiment described in Sec. 3.3.

We measured the radial profile of the electron density and the electron temperature and the time evolution of the ion saturation current using a Langmuir probe in the production region ($z = 0.57$ m) and in the test region ($z = 1.53$ m). The probe diameter and length are 0.35 mm and 1.0 mm, respectively. To obtain probe voltage-current characteristics, we applied a 250 Hz sawtooth voltage from -180 V to 50 V to the probe. These data were obtained in different shots for production and test regions to avoid influence of probe shadow.

3. Results and Discussion

3.1 Radial profile of the electron density and the electron temperature

To investigate the plasma parameters, we measured radial profiles of the electron density and the electron temperature at $B_{MCT} = 0.3$ T as shown in Fig. 3. The circles and the diamonds indicate the profiles in the production region ($z = 0.57$ m) and in the test region ($z = 1.53$ m), respectively. An overdense, $n_e > 7.5 \times 10^{16} \text{ m}^{-3}$, plasma was successfully obtained.

The electron density in the test region was lower than that in the production region. Typical electron density was $5 \times 10^{17} \text{ m}^{-3}$ and the electron temperature was 4 eV in the test region. The radius of plasma estimated from the den-

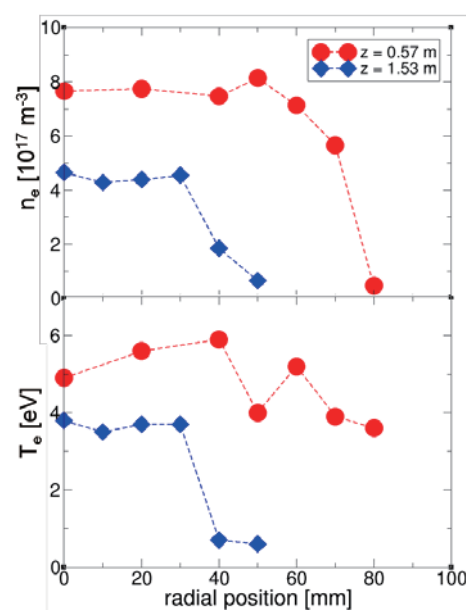


Fig. 3 Radial profile of (top) electron density and (bottom) electron temperature.

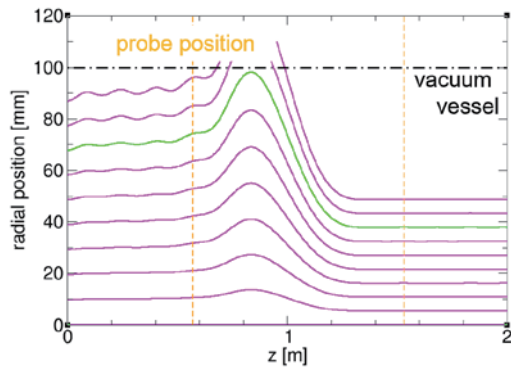
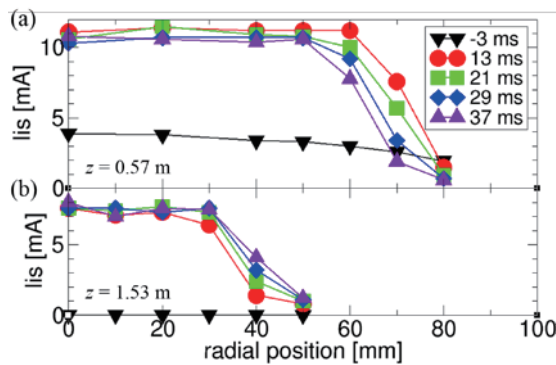


Fig. 4 Trace of magnetic field lines in NUMBER.


 Fig. 5 Time evolution of the radial profile of the ion saturation current (I_{is}) (a) in the production region and (b) in the test region.

sity profile was 60–70 mm in the production region and 30–40 mm in the test region.

Figure 4 shows the magnetic field lines calculated for $B_{MCT} = 0.3$ T. The radius of vacuum vessel wall is 100 mm, so the plasma on the magnetic field lines that spread out to 100 mm in the radial direction is isolated between the production region and the test region. The green line represents the outermost magnetic field line connecting the production region and the test region. The radial positions at probe positions ($z = 0.57$ m, 1.53 m) on the green line are about 70 mm and 40 mm. These are consistent with the radial profile of the electron density shown in Fig. 3.

Figure 5 shows the time evolution of the radial profile of the ion saturation current (I_{is}) in the production region and in the test region. Here, we discuss the B_{MCT} decreasing phase ($t > 13$ ms). The phenomenon that the ion saturation current increased between $t = -3$ ms and $t = 13$ ms will be discussed in the next section. As shown in Fig. 6, the radial position of the outermost field line at $z = 1.53$ m spread out with time because the magnetic field strength in the test region became weaker. Therefore, ion saturation current at $r = 40$ mm gradually increased, namely the radius of plasma was expanded. These results indicated that plasma was transported along the magnetic field as we expected.

The plasma cross section in the test region becomes

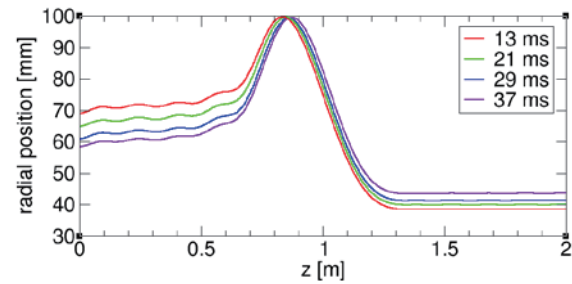


Fig. 6 Time evolution of the outermost field line.

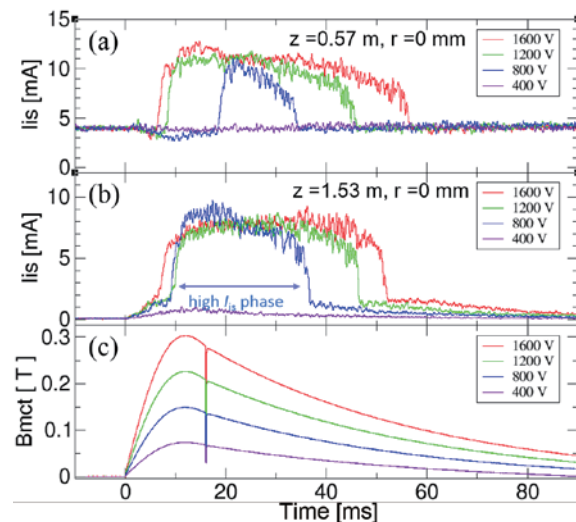


Fig. 7 Time evolution of ion saturation current (a) in the production region and (b) in the test region. (c) Time evolution of magnetic field strength in the test region.

smaller than that in the production region. If the plasma is completely transported along the magnetic field lines, the electron density in the test region should be larger than that in the production region. However, these experimental results show that lower density in the test region than that in the production region. This is caused by radial diffusion.

The radius $r = 40$ mm of plasma column in the $B_{MCT} = 0.3$ T test region satisfied our requirement well. The achieved density and temperature matched to requirements within a few factors. In the following subsections, charging voltage and gas pressure dependences are described for better understanding of plasma production.

3.2 Charging voltage dependence

To investigate the magnetic field configuration dependence of plasma production and parallel transport, we measured the ion saturation current (I_{is}) in various charging voltages. The charging voltage of capacitor bank (V_{EC}) was varied from 400 V to 1600 V. Figure 7 shows time evolution of the ion saturation current in the production region and in the test region and that of magnetic field strength in the test region (B_{MCT}). The ion saturation current in the test region began to rise gradually at the beginning of a coil

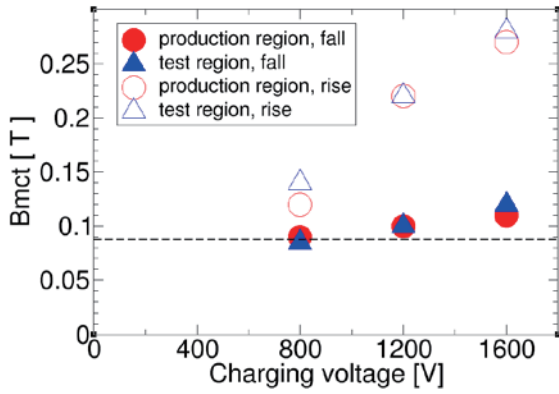


Fig. 8 Magnetic field strength at the rise/fall time of the high I_{is} phase as a function of the charging voltage.

current pulse. Large increase in the ion saturation current (high I_{is} phase) was observed both in the production and the test regions except for $V_{EC} = 400$ V case. The duration of the high I_{is} phase became longer as the charging voltage became higher. The magnitude of the ion saturation current in the high I_{is} phase was unchanged under the conditions of $V_{EC} = 800$ V, 1200 V, and 1600 V. On the other hand, in the case of $V_{EC} = 400$ V, the high I_{is} phase was not observed. In this case, the magnetic field strength in the test region did not exceed 0.0875 T.

Figure 8 shows the magnetic field strength at the rise/fall time of the high I_{is} phase, which are determined by the onset/end of high I_{is} phase just after/before the rapid change of I_{is} , as a function of the charging voltage. The ion saturation current suddenly decreased at $B_{MCT} \approx 0.0875$ T (dashed line) in the B_{MCT} decreasing phase. The magnetic field strength at the rise time became higher as the charging voltage became higher. This might be because the increasing rate of the magnetic field strength was larger for the higher charging voltage. The delay of the rise time from the time that the magnetic field strength exceeded 0.0875 T was rather shorter for the higher charging voltage.

From these results, we suspected that the electron cyclotron resonance (ECR) occurred and the plasma was generated in the test region as well as in the production region. From the dispersion relation in cold uniform plasma, microwave of frequency 2.45 GHz can not propagate in the condition, in which the magnetic field strength was smaller than 0.0875 T for the electron density, $8.0 \times 10^{17} \text{ m}^{-3}$. Therefore, we considered no microwaves propagate beyond the ECR position in the production region ($z = 0.6$ m). However, from the experimental results, the microwave seems to be propagated to the test region. There is a report that microwaves can be propagated in a cylindrical chamber filled with uniform magnetized plasma like in a coaxial waveguide [6]. In the future, we will investigate the microwave propagation.

3.3 Gas pressure dependence

Time evolution of the ion saturation current (I_{is}) in the

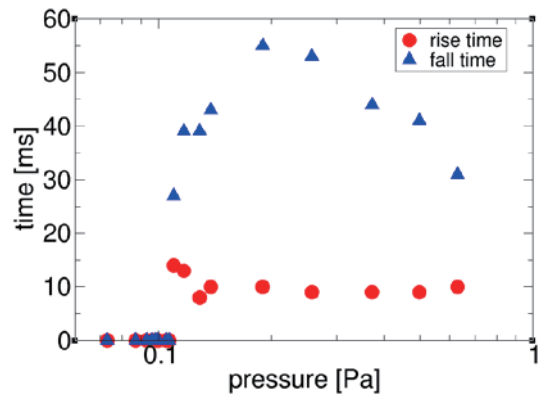


Fig. 9 The rise/fall time of the high I_{is} phase in the test region as a function of the gas pressure.

test region was investigated for various gas pressures from 7.3×10^{-2} Pa to 6.3×10^{-1} Pa. These experiments were performed on the condition of $V_{EC} = 1600$ V. It was found that appearance and duration of the high I_{is} phase depended on the gas pressure. Figure 9 shows the rise/fall time of the high I_{is} phase as a function of the gas pressure. In the case of $p < 1.1 \times 10^{-1}$ Pa, the high I_{is} phase was not observed. When the gas pressure exceeded 1.1×10^{-1} Pa, the high I_{is} phase was observed. Up to the gas pressure of 1.9×10^{-1} Pa, duration time of the high I_{is} phase became longer as the gas pressure became higher. For the gas pressure $p > 1.9 \times 10^{-1}$ Pa, the time of the high I_{is} phase became shorter as the gas pressure became higher. The maximum duration time was obtained at $p = 1.9 \times 10^{-1}$ Pa.

From these results, it is found that the gas pressure affects the phenomenon of the high I_{is} phase. We studied the relationship between the ionization collision frequency ν_i and plasma confinement time L/C_s . Here, C_s and L are the ion sound velocity and the device length. When $L/C_s > \nu_i^{-1}$, electrons efficiently ionize neutrals. We assumed the electron temperature is 4 – 6 eV, then L/C_s and ν_i^{-1} are almost comparable at $p = 2 \times 10^{-1}$ Pa. The relationship between these values may possibly be important for whether or not the high I_{is} phase occurs.

4. Conclusions

The radial profile of the electron density and the electron temperature were evaluated using a Langmuir probe in a connected linear device, NUMBER. In the test region, an electron density of $5 \times 10^{17} \text{ m}^{-3}$ and an electron temperature of 4 eV were achieved. The plasma was transferred between the production region and the test region along the magnetic field lines. A magnetic field configuration dependence and a gas pressure dependence of the ion saturation current (I_{is}) were investigated. Rapid increase and rapid decrease in the ion saturation current (high I_{is} phase) were observed both in the production region and the test region. Possibility of an unexpected plasma production in the test region is suggested.

Acknowledgment

This work was partly supported by JSPS/MEXT of Japan, Kakenhi 26420848 & 24246152.

- [1] S. Inagaki *et al.*, Jpn. J. Appl. Phys. **36**, 3697 (1997).
- [2] N. Krause *et al.*, Rev. Sci. Instrum. **73**, 3474 (2002).

- [3] J. H. Harris *et al.*, Nucl. Fusion **44**, 279 (2004).
- [4] K. Yamazaki *et al.*, J. Plasma Fusion Res. SERIES **8**, 1044 (2009).
- [5] M. Tanaka *et al.*, J. Phys. Soc. Jpn. **60**, 1600 (1991).
- [6] I. Watanabe, H. Nishimura and S. Matsuo, Jpn. J. Appl. Phys. **34**, 3675 (1995).